Phyllobacterium Calauticae Sp. Nov. Isolated From a Microaerophilic Veil Transversed by Cable Bacteria in Freshwater Sediment

Jamie J.M. Lustermans
Aarhus University

Jesper Jensen Bjerg
Aarhus University

Andreas Schramm (andreas.schramm@bio.au.dk)
Aarhus University https://orcid.org/0000-0002-7614-9616

Ian P.G. Marshall
Aarhus University

Research Article

Keywords: chemotaxis, gradient, microaerophile, motility, oxic-anoxic interface, sulfide

Posted Date: July 22nd, 2021

DOI: https://doi.org/10.21203/rs.3.rs-731961/v1

Version of Record: A version of this preprint was published at Antonie van Leeuwenhoek on September 7th, 2021. See the published version at https://doi.org/10.1007/s10482-021-01647-y.

Confidential Information:
Manuscript for submission to Antonie van Leeuwenhoek, 17 July 2021

Phyllobacterium calauticae sp. nov. isolated from a microaerophilic veil transversed by cable bacteria in freshwater sediment

Jamie J.M. Lustermans[1], Jesper J. Bjerg[1,2], Andreas Schramm[1]*, and Ian P.G. Marshall[1]

[1] Section for Microbiology, Center for Electromicrobiology, Department of Biology, Aarhus University, Aarhus, Denmark

[2] Microbial Systems Technology Excellence Centre, University of Antwerp, Wilrijk, Belgium

***corresponding author:**

Section for Microbiology, Center for Electromicrobiology, Department of Biology, Aarhus University, Ny Munkegade 114, Building 1540, 8000 Aarhus C, Denmark

Email: andreas.schramm@bio.au.dk; Phone: +45 60 20 26 59

ORCID identifiers

Jamie J.M. Lustermans: 0000-0001-8657-3771

Jesper J. Bjerg: 0000-0003-3536-2928

Andreas Schramm: 0000-0002-7614-9616

Ian P.G. Marshall: 0000-0001-9264-4687

Acknowledgements

We thank Susanne Nielsen and Lars B. Pedersen for their work and support in the molecular and microbiological laboratories; Pia Bomholt Jensen for excellent SEM images; and Ronny Mario Baaske for care of the cable bacteria enrichments. This research was supported by the Danish National Research Foundation (DNRF136) and the Carlsberg Foundation (CF19-0666).

Abstract

Microaerophilic veils of swimming microorganisms form at oxic-anoxic interfaces, most commonly described in sediments where sulfide diffusing out from below meets oxygen diffusing in from the water phase. However, distinctive microaerophilic veils form even when there is a gap between the sulfide and O_2 fronts, i.e., a suboxic zone, and suggest that the organisms inhabiting these veils can use electron donors other than sulfide. Suboxic zones are found for example in sediment where cable bacteria spatially separate sulfide and O_2 by up to several centimetres. Here we describe the extraction of microorganisms from a microaerophilic veil that formed in cable-bacteria-enriched freshwater sediment using a glass capillary, and the subsequent isolation of a motile, microaerophilic, organoheterotrophic bacterium, strain R2-JL^T, unable to oxidize sulfide. Based on phenotypic, phylogenetic, and genomic comparison, we propose strain R2-JL^T as a novel *Phyllobacterium* species, *P. calauticae* sp. nov.. The type strain is R2-JL^T (=LMG 32286^T =DSM 112555^T). This novel isolate confirms that a wider variety of electron donors, including organic compounds, can fuel the activity of microorganisms in microaerophilic veils.

Keywords

chemotaxis, gradient, microaerophile, motility, oxic-anoxic interface, sulfide

Introduction

Oxic-anoxic interfaces (OAIs) are present in all environments where oxygen is consumed faster than replenished, such as aquatic sediments, and are home to microbial communities that are well adapted to micro-oxic conditions (Brune *et al.*, 2000; Thar & Kühl, 2002; Thar & Fenchel, 2005). These communities frequently form a microaerophilic veil right at the OAI, with oxygen completely depleted behind the veil (Thar & Fenchel, 2005; Scilipoti *et al.*, 2021). Specific low concentrations of oxygen are actively sought out by the microorganisms, which indicates chemotaxis towards the preferred oxygen concentration (Barbara & Mitchell, 1996; Thar & Fenchel, 2005). Microaerophilic veils typically form at the OAI where oxygen and sulfide meet, and thus the characterization of veil microorganisms has been focused on sulfide-oxidizing bacteria (Thar & Kühl, 2002; Muyzer *et al.*, 2005).

However, microaerophilic veils form even when sulfide and oxygen are separated by a layer without detectable oxygen and sulfide, a suboxic zone (Froelich *et al.*, 1979; Berner, 1981). Such suboxic layers are found, for example, in sediments with active cable bacteria (Nielsen *et al.*, 2010; Pfeffer *et al.*, 2012; Schauer *et al.*, 2014). Cable bacteria are up to centimetres-long, multi-cellular, filamentous, sulfide-oxidizing bacteria (Pfeffer *et al.*, 2012). They spatially separate their metabolic redox half reactions by transporting electrons from sulfide oxidation to the oxic surface sediment, where oxygen is reduced (Pfeffer *et al.*, 2012), and thus create a suboxic zone up to several centimetres wide (Schauer *et al.*, 2014). While sulfide and oxygen never directly meet in these zones, microaerophilic veils form along the OAI of cable bacteria-induced suboxic zones (Bjerg *et al.*, 2016; Scilipoti *et al.*, 2021). This suggests that organisms in these microaerophilic veils use electron donors other than sulfide. The aim of this study was to isolate and characterize bacteria from such a veil, with a focus on chemoorganotrophs. To extract bacterial cells from the veil, we adapted a glass capillary technique, used for molecular identification of veil bacteria (Muyzer *et al.*, 2005), and proceed here to describe a novel species of the genus *Phyllobacterium*.

Materials and methods

Isolation and cultivation of bacteria

For the visualization of the microaerophilic veil, an in-house designed "trench slide" was used (Bjerg *et al.*, 2016; 2018; Thorup *et al.*, 2021). The glass slide chamber system was adapted by raising the coverslip, which was done by adding 2 broken parts of a glass coverslip on each side of the sediment chamber (Figure 1). The glass fragments were anchored in place with Vaseline. The trench slide allows space for sediment in the middle, a layer of water that is increased slightly by the small adaptation, and has a glass surface around the central sediment space to facilitate light passing through. Oxygen diffuses in from the side, while sulfide and other compounds diffuse from the sediment into the water layer, creating geochemical gradients.

Sediment was derived from a pond at Aarhus University campus (Vennelyst Park), Denmark (56.164672, 10.207908), at a water depth of 0.5-1 m and stored with overlying water at 15 °C for two weeks. After storage, the sediment was homogenized, sieved (pore size: 0.5 mm), and autoclaved at 121 °C for 20 min in 2 L bottles, cooled down to 15 °C, homogenized and distributed into 50 ml Falcon tubes. Inoculation of the sediment was performed with a pre-grown enrichment culture (at 15 °C) of a single cable bacterium species (Thorup *et al.*, 2021). After 2 weeks a clump of sediment (~5 mm^3) was transferred into the modified trench slide. The trench slide was incubated in a humid environment at 15 °C over night.

With a phase-contrast microscope at 50× magnification (Leica 020-507.010, Germany) the microaerophilic veil that formed in the glass trench slide was localized. Cells were reproducibly extracted from the microaerophilic veil with a handmade glass capillary (diameter: 80-150 µm, sterilised by 1.5 h of UV-radiation). Through use of the microscope and a micromanipulator (Unisense A/S, Denmark), we kept control over the location of extraction. The extracted volume was regulated by connecting the capillary to a flowrate-controlled (100-200 µl min^{-1}), programmable syringe pump (TSE Systems, Germany) that held a 10 ml syringe filled with milliQ water to prevent introduction of bubbles. The capillary was inserted by wedging the capillary in between the glass slide and its coverslip

(Figure 1). When the veil re-established itself after forced movement from water flow pressure, cells were visibly sucked into the capillary. The flow rate and location was adapted during extraction to exclude cable bacteria and sediment particles. Extracted cells were transferred into a PCR tube and diluted 1:1 with 1:10 diluted R2A (18 g l^{-1}, Sigma-Aldrich, Germany) and kept at 4 °C for approximately 5-15 minutes until inoculation.

Nutrient broth (8 g NB l^{-1}, Scharlau, Spain), R2A, and Tryptic Soy Broth (30 g TSB l^{-1}, Scharlau) plates (15 g agar l^{-1}, Scharlau) were inoculated with 2-10 µl extract, as well as with 1:10, 1:100, and 1:1000× diluted extract (in R2A). All plates were incubated at 15 °C in the dark. After 2 weeks, distinct colonies were selected and used as inoculum. The novel isolate originated from a 1:1000 diluted inoculum grown for 7 days on NB agar plates. Liquid cultures of the novel isolate were grown in NB with a headspace of at least 50% atmospheric air.

Taxonomy screen based on 16S rRNA

After distinct colonies were visible on the second generation plates a colony PCR was performed to obtain an initial taxonomic classification. Samples were PCR amplified for the 16S rRNA gene with primers 27F/1492R (Lane, 1991), DNA concentrations were determined with a Nanodrop (Thermo Fisher), and sequencing of the 16S rRNA gene was performed by Macrogen Europe B.V. (Sanger sequencing). Taxonomic classification of the isolates was determined after trimming off the primer and poor quality bases determined with Chromas (Technelysium). Sequences were used as query sequences with nucleotide BLAST (Camacho *et al.*, 2009) against the Nucleotide collection (nr/nt) database, excluding uncultured/environmental sample sequences.

Genome sequencing, assembly and annotation

Genomic DNA was extracted from third generation colonies with a DNeasy PowerLyzer PowerSoil DNA Isolation Kit (Qiagen), concentrations and length distribution were scanned using the Agilent 4200 TapeStation with a Genomic DNA ScreenTape in the size range of 200 to >60,000 bp (Agilent

Technologies), then a Nextera XT DNA Library Preparation kit (Illumina) was used, and 2×300bp paired-end sequencing using the Illumina MiSeq platform was performed in-house following the standard Illumina protocol for MiSeq reagent kit v3. Raw sequence quality was assessed using FastQC v0.11.5 (Wingett & Andrews 2018) before and after trimming with Trimmomatic v.0.39 (Bolger *et al.*, 2014): headcrop 20; sliding window 4:20; minimum length 100bp; adapter trimming with parameters 2:40:15. Trimmed paired-end and non-paired reads were *de novo* assembled with SPAdes v3.14.1 (Bankevich *et al.*, 2012) with: default k-mers 21, 33, 55, 77, 99, 127; the option careful; automatic coverage cutoff. Completeness, contamination, and quality were estimated with CheckM v1.1.3 (Parks *et al.*, 2015) and Quast v4.3 to determine the quality of the final assembly. Using Prokka v1.14.5 (Seemann 2014) with a minimal contig length of 300, first a genus database was generated based on *Phyllobacterium* genomes (*P. myrsinacaerum* DSM 5892^T*, P. sp* 628*, P. bourgognense* 21-35^T). This curated database was used as primary annotation source against which the genome of R2-JL^T was searched using protein-protein BLAST within the Prokka pipeline. Additionally, protein-encoding genes were also annotated through BlastKOALA and KEGG Mapper (Kanehisa and Goto, 2000; Kanehisa *et al.*, 2016; Kanehisha 2019). The web services were also used to determine absence or presence of metabolic pathways.

Taxonomic and additional genomic analyses

To determine the taxonomy of the strain, all genomes designated to the genus *Phyllobacterium* were downloaded from NCBI and compared by calculating average nucleotide identities using FastANI v1.32 (Jain *et al.*, 2018) with minimal fragment size set to 50. Estimates from FastANI were checked by running ANI calculations using the web service (http://enve-omics.ce.gatech.edu/ani/; Goris *et al.*, 2007) between the sample and *P. myrsinacearum* DSM 5892^T. Phylogenetic marker genes were identified in all the genomes by GTDB-Tk v1.4.0 (Chaumeil *et al.*, 2019; Parks *et al.*, 2018; Matsen *et al.*, 2010; Jain *et al.*, 2019; Eddy, 2011), which uses Prodigal (Hyatt *et al.*, 2010) for this purpose. Using GTDB-Tk align, the identified 120 marker genes were translated to protein sequences and a

concatenated multiple sequence alignment was made. A maximum likelihood tree with 1000 bootstrap replicates was calculated from this data with FastTree v2.1.11 SSE3 (Price *et al*., 2010, 2009). The tree was rooted with *Mesorhizobium loti* LMG 6125^{T}.

MEGA X (Kumar *et al.*, 2018) alignment with Clustal ω (Sievers *et al.*, 2011) and BLAST were used to determine similarities between the cytochrome *bd* complexes of *Escherichia coli* and strain R2-JL.

Physiological testing

Cells were harvested from plates to perform three API (20E, 20NE, ZYM; BioMérieux) tests and to inoculate a Biolog Gen III microplate (Agilent). The API tests were performed as described in the manual, with exception of the incubation that was executed in the dark at room temperature for 24-72 hours depending on the test. The Biolog Gen III plate was measured with a FLUOstar Omega microplate reader which makes use of their Omega 3.00 R2 software (BMG Labtech, France). Gram-staining was performed on liquid cultures. An OF Hugh-Leifson test for glucose fermentation was performed with additional 0.5 g L^{-1} yeast extract and 10 g L^{-1} glucose added before autoclaving. Growth at different temperatures was tested in duplicate or triplicate where a 3-7 day old single colony of R2-JL was aseptically streaked on fresh NB plates. Plates were incubated under dark conditions at 0.5, 4, 15, 22, 30, 35, 37, 40 and 42 °C, and checked regularly for growth or dehydration up to 2 weeks after inoculation. To test for catalase presence one or two successive drops of cold hydrogen peroxide were dripped onto a three- and a five-day-old colony.

Light microscopy

A 0.5 ml sample of shaken liquid culture of R2-JL was added to a normal glass microscopy slide and covered with a coverslip, this was performed in duplicate at 22 °C. Microaerophilic veil formation was observed for 5-10 min before capturing pictures. The microaerophilic veil formation was captured using phase contrast on a ZEISS Observer Z1 (Zeiss, Göttingen, Germany) inverted microscope with PALM automated stage. Images were taken at 100× magnification, with Zen Black edition (Zeiss).

Scanning Electron Microscopy (SEM)

Liquid cultures of 3-5 days old were diluted (1:2 in milliQ), air dried onto a silicon wafer and sputtered with 2 nm of platinum with a Leica EM SCD 500 platinum coater (Leica Microsystems, Wetzlar, Germany) at 35 mA under argon atmosphere. Wafers were subsequently analysed with a high vacuum SEM: Versa 3D, dual beam system (FEI, Oregon, USA). Scanning parameters: 13 pA and 5 kV.

Results and Discussion

We isolated 29 bacteria from freshwater sediment containing a single species of cable bacteria; *Ca.* Electronema aureum. The bacteria were extracted from a microaerophilic veil that formed in the modified trench slide, filled with freshwater sediment where cable bacteria thrive (Thorup *et al.*, 2021). Five of the isolates belonged to the genus *Phyllobacterium*. All five isolates appeared to be identical on a genomic level with a FastANI score greater than 99.99%. We therefore focused our efforts on one of these isolates: R2-JL.

Morphological and Physiological analyses

Phyllobacterium sp. R2-JL, the isolated strain, was found to be a Gram-negative, catalase-positive bacterium that is motile with at least one (sub)polar flagellum. Cells were slightly curved, rod-shaped, and approx. 2 × 0.6 µm in size (Fig. 2a). The cells formed a microaerophilic veil even in pure culture (Fig. 2b), suggesting chemotactic behaviour specific to oxygen. The isolate did not reduce nitrate, and was OF-test negative suggesting that it cannot ferment glucose. Strain R2-JL can physiologically be distinguished from all other phyllobacteria based on its ability to grow on D-raffinose, arabinose and the absence of growth on quinic acid (Table 1). It can be distinguished from its currently closest relative *P. myrsinacearum* by growth of R2-JL on α-D-lactose, D-melibiose, D-raffinose, glucuronamide, N-acetyl-D-galactosamine, and by absence of growth of R2-JL on α-keto-glutaric acid, D-gluconic acid, D-

glucose-6-phosphate, D-lactic acid methyl ester, γ-amino-butyric acid, glycerol, inosine, L-lactic acid, L-serine, N-acetyl-β-D-mannosamine and the absence of urease (Table 1).

R2-JL appears to grow exclusively on organic compounds, specifically on hexoses in mono-, di- or polysaccharide form, like glucose, sucrose, and pectine, L-rhamnose, and esculine (Table S1), which are found commonly in plants. The freshwater sediment where strain R2-JL originates from has an input of dead or partially degraded plant material, explaining the access to these carbon compounds. The novel strain is currently the only *Phyllobacterium* that has been isolated from sediment, where all other species have been isolated from plant rhizospheres, root or leaf nodules of tropical ornamental plants (Knösel, 1962) (Table 1). Until now, only 2 species have been identified that were not isolated from nodules: *P. phragmitis* (Liang *et al.*, 2019) and *P. catacumbae* (Jurado *et al.*, 2005).

Phylogenetic analyses and genomic characteristics

The 16S rRNA gene sequence of R2-JL is identical to that of *P. myrsinacearum*, and highly identical (>98%) to 5 other phyllobacteria (Table 1). The genomes of R2-JL and *P. myrsinacearum* have an ANI of 92.64% and all other *Phyllobacterium* species are less than 81% identical to R2-JL (Table 1, Table S2). These results were suggestive of a novel species of *Phyllobacterium* for our strain (Richter & Rosselló-Móra, 2009; Jain *et al.*, 2018), which clustered within the *Phyllobacterium* genus (Fig. 3). Figure 3, like Table 1, shows that *P. myrsinacearum* DSM 5892^T is the closest known relative to the novel strain. It also clustered all *P. myrsinacearum* in a different cluster than R2-JL (bootstrap value >99% out of 1000 iterations), except for *P. myrsinacearum* AN3 which is in yet a third cluster.

Evidence from phylogenetic, genomic and phenotypic analyses, strengthened by its distinct isolation source that is free of living plants, and its apparent free-living lifestyle, leads to the conclusion that strain R2-JL belongs to a novel species within the genus *Phyllobacterium*. As the novel bacterium was isolated from a microaerophilic veil (in freshwater sediment), we propose the name *Phyllobacterium calauticae* sp. nov., with the type-strain R2-JL.

226 The genome of *P. calauticae* R2-JL^T consists of 31 contigs, is 5,288,098 bp in size with a G+C content
227 of 59.12%, and completeness was estimated to be 100% with 0.00% contamination. Gene prediction
228 and annotation identified 5111 putative protein-coding genes, whereof 1119 (21.69%) are
229 hypothetical proteins. Of these, 2768 (54.2%) could be annotated with BlastKOALA (Kanehisha *et al.*,
230 2016).
231
232 Genomic and phenotypic insights into R2-JL^T's ecophysiology and lifestyle
233 In agreement with phenotypic data, we find a flagellar assembly pathway (02035), several genes
234 related to chemotaxis, and aerobic respiration pathways in the genome of *P. calauticae* R2-JL^T.
235 Chemotaxis related genes that were found are *che*Y that is a flagellar switch (Szurmant *et al.*, 2003;
236 Miller *et al.*, 2009), PA1976 which is used for swarming and biofilm formation (Hsu *et al*, 2008), and
237 *reg*AB that is used to sense redox signals (Emmerich *et al.*, 2000). Presence of sensitivity towards redox
238 signals, the veil formation, a flagellar and swarming switch, all indicate that R2-JL^T has a chemotaxis
239 towards oxygen.
240 For energy conservation, R2-JL^T has an F-type ATPase (M00157), and a respiratory electron transport
241 chain, including NADH quinone oxidoreductase (M00144), succinate dehydrogenase (M00149),
242 ubiquinone-cytochrome *c* reductase and oxidase (M00151, M00155), and likely both a low affinity
243 terminal oxidase (cytochrome *o* ubiquinol oxidase, M00417), and a high affinity oxidase (cytochrome
244 *bd* ubiquinol oxidase (*cyd*AB, M00153)). R2-JL^{T}s CydA resembles that of *Escherichia coli* K-12
245 (protein_id: QHB69574.1) based on alignments (data not shown) and BLASTp comparisons (59.4%
246 identity). *E. coli*'s cytochrome *bd* complex is described as a very high affinity terminal oxidase (K_m 3-8
247 nM O_2) and it likely facilitates growth under low- or micro-oxic conditions (Rice & Hempfling, 1978;
248 D'mello *et al.*, 1996; Borisov *et al.*, 2011). Thus, the cytochrome *bd* complex of *P. calauticae* R2-JL^T
249 potentially has a high affinity for oxygen and may enable micro-aerobic respiration of R2-JL^T under the
250 micro-oxic conditions that are found in the veil. Neither genomic nor physiological data showed

indications of an anaerobic metabolism such as nitrate reduction or fermentation to support life on the anoxic side of the veil.

On the electron donor side, there is good phenotypic evidence that R2-JL^T utilizes a broad spectrum of different organic compounds (Table 1, Table S1). On the other hand, there are no phenotypic or genomic indications for the use of sulfide as electron donor, and both Sox and rDSR pathways are absent. Thus, *P. calauticae* R2-JL^T was not only isolated from a microaerophilic veil, but seems to be a microaerophile that uses organic compounds (for example plant-derived hexoses) for its metabolism, in contrast to most other bacteria described from microaerophilic veils, which make use of the sulfide-oxygen gradient (Thar & Fenchel, 2002; Muyzer *et al.*, 2005).

Species of *Phyllobacterium* are usually associated with plants (Knösel, 1962), or have at least been isolated from root or leaf nodules (Table 1). Two *Phyllobacterium* species, *P. trifolii* (Valverde *et al.*, 2005) and *P. sophorae* (Jiao *et al.*, 2015), possess the genes necessary for nodule formation (*nod*ACD) or nitrogen fixation (*nif*DKH). In contrast, the genome of *P. calauticae* R2-JL^T did not contain any of the plant signalling pathways (MAPK), *nod*ACD genes, *nif*DKH genes, or plant-pathogen interaction pathways. This strongly indicates that R2-JL^T lacks the ability to form symbiotic, commensal or pathogenic interactions with plants and belongs to the free-living *Phyllobacterium* (Safronova *et al.*, 2018).

Conclusion

P. calauticae R2-JL^T (= LMG 32286^T, = DSM 112555^T), the first *Phyllobacterium* from sediment, is an organoheterotrophic, aerobic bacterium, isolated from a microaerophilic veil that formed in cable-bacteria-enriched freshwater sediment. With its motility, chemotaxis, and presumably high affinity terminal oxidase, R2-JL^T appears adapted to the moving counter-gradients typical of a microaerophilic veil, where oxygen overlaps with reduced organic compounds diffusing from the organic-rich, anoxic sediment. Ultimately, these results expand our view of the bacteria in microaerophilic veils and the compounds they utilise other than sulfide.

Description of *P. calauticae* R2-JL^T (type strain)

Phyllobacterium calauticae (ca' lau. ti. cae N.L. gen. n. *calauticae* of *calautica*; a headdress or turban reaching to the shoulders i.e. veil, from which the type strain was isolated).

Cells are Gram-stain-negative, aerobic slightly curved rods (2 µm x 0.6 µm) that are motile by at least one (sub)polar flagellum. They form mucoid milky-white undulate-shaped colonies (2-5 mm diameter) and often present with transparent edges and radial whiteness emerging from the centre, after 48 h of incubation at 15 °C. *P. calauticae.* R2-JL^T is catalase positive, and OF-test negative for glucose, but arabinose and glucose showed weak growth. Salinity is tolerated to at least 4.0% (w/v) NaCl, it can grow at a pH of at least 5.0-7.2, and at a temperature of 0.5-37 °C, with weak growth at 0.5, 4, and 37 °C. The G+C content of the genomic DNA is 59.12%.

Type strain R2-JL^T (=LMG 32286) was isolated from a microaerophilic veil forming in a microscopy chamber with freshwater sediment that contained a single strain enrichment of cable bacteria (Thorup *et al.*, 2021). The extracted sample was collected in March 2019 and cultivated until a pure culture was reached in June 2019. The accession number for *P. calauticae* R2-JL^{T}s draft genome sequence is JAGENB000000000.

Declarations

Funding. This research was supported by the Danish National Research Foundation (DNRF136) and the Carlsberg Foundation (CF19-0666).

Conflicts of interest/Competing interests. No conflicts of interest to declare.

Availability of data and material. *P. calauticae* R2-JL^T is available from BCCM/LMG Gent, Belgium (LMG 32286^T) and DSMZ, Braunschweig, Germany (DSM 112555^T). The draft genome sequence is available from NCBI under the accession number JAGENB000000000.

Code availability. Not applicable.

Authors' contributions. JL, JB, AS, and IM conceived and designed the study; JL and AS performed research; JL analysed data; JL, JB, and IM contributed new methods or models; JL, AS, and IM wrote the paper; all authors have read and approved the final manuscript.

References

Bankevich A, Nurk S, Antipov D, Gurevich AA, Dvorkin M et al (2012) SPAdes: a new genome assembly algorithm and its applications to single-cell sequencing. J Comput Biol 19(5):455–477. https://doi.org/10.1089/cmb.2012.0021

Barbara GM, Mitchell JG (1996) Formation of 30- to 40-Micrometer-Thick Laminations by High-Speed Marine Bacteria in Microbial Mats. Appl Environ Microbiol 62(11):3985-3990. DOI: 10.1128/aem.62.11.3985-3990.1996

Berner RA (1981) A new geochemical classification of sedimentary environments. J Sed Petrol 51(2):0359-0365. https://doi.org/10.1306/212F7C7F-2B24-11D7-8648000102C1865D

Bjerg JT, Boschker HT, Larsen S et al (2018) Long-distance electron transport in individual, living cable bacteria. PNAS 115(22), 5786-5791. https://doi.org/10.1073/pnas.1800367115

316 Bjerg JT, Damgaard LR, Holm SA, Schramm A, Nielsen LP (2016) Motility of electric cable bacteria. App
317 Environ Microbiol 82(13), 3816–3821. https://doi.org/10.1128/AEM.01038-16

318 Bolger AM, Lohse M, Usadel B (2014) Trimmomatic: a flexible trimmer for Illumina sequence data.
319 Bioinformatics 30(15):2114–2120. https://doi.org/10.1093/bioinformatics/btu170

320 Borisov VB, Gennis RB, Hemp J, Verkhovsky MI (2011) The cytochrome *bd* respiratory oxygen
321 reductases. Biochim Biophys Acta 1807:1398-1413. https://doi.org/10.1016/j.bbabio.2011.06.016

322 Brune A, Frenzel P, Cypionka H (2000) Life at the oxic-anoxic interface: microbial activities and
323 adaptations. FEMS Microbiol Rev 24: 691-710. https://doi.org/10.1111/j.1574-6976.2000.tb00567.x

324 Camacho C, Coulouris G, Avagyan V et al. (2009) BLAST+: architecture and applications. BMC
325 Bioinformatics 10, 421. https://doi.org/10.1186/1471-2105-10-421

326 Chaumeil PA et al (2019) GTDB-Tk: A toolkit to classify genomes with the Genome Taxonomy
327 Database. Bioinformatics, btz848

328 D'mello R, Hill S, Poole RK (1996) The cytochrome *bd* quinol oxidase in *Escherichia coli* has an extremely
329 high oxygen affinity and two oxygen-binding haems: implications for regulation of activity in vivo by
330 oxygen inhibition. Microbiology 142 755-763

331 Flores-Félix JD, Carro L, Velázquez E, Valverde Á , Cerda-Castillo E, García-Fraile P, Rivas R (2013)
332 *Phyllobacterium endophyticum* sp. nov., isolated from nodules of *Phaseolus vulgaris*. Int J Syst Evol
333 Microbiol 63:821–826

334 Emmerich R, Hennecke H, Fischer HM (2000) Evidence for a functional similarity between the two-
335 component regulatory systems RegSR, ActSR, and RegBA (PrrBA) in alpha-Proteobacteria. Arch
336 Microbiol 174:307-13. DOI:10.1007/s002030000207

337 Froelich PN, Klinkhammer GP, Bender ML, Luedtke NA, Heath GR, Cullen D, Dauphin P, Hammond D,

Goris J, Konstantinidis KT, Klappenbach JA, Coenye T, Vandamme P, Tiedje JM (2007) DNA-DNA hybridization values and their relationship to whole-genome sequence similarities. DOI: 10.1099/ijs.0.64483-0

Hsu JL, Chen HC, Peng HL, Chang HY (2008) Characterization of the histidine-containing phosphotransfer protein B-mediated multistep phosphorelay system in *Pseudomonas aeruginosa* PAO1. J Biol Chem 283:9933-44. DOI:10.1074/jbc.M708836200

Hyatt D, Chen G-L, LoCascio P, Land M, Larimer F, Hauser L (2010) Prodigal: prokaryotic gene recognition and translation initiation site identification. BMC Bioinformatics 11:119. doi: 10.1186/1471-2105-11-119

Jain C, Rodriguez-R LM, Phillippy AM et al (2018) High throughput ANI analysis of 90K prokaryotic genomes reveals clear species boundaries. Nat Commun. doi: 10.1038/s41467-018-07641-9

Jiao YS, Yan H, Ji ZJ, Liu YH, Sui XH, Zhang XX, Wang ET, Chen WX, Chen WF (2015) *Phyllobacterium sophorae* sp. nov., a symbiotic bacterium isolated from root nodules of *Sophora flavescens*. Int J Syst Evol Microbiol 65:399–406

Jurado V, Laiz L, Gonzalez JM, Hernandez-Marine M, Valens M, Saiz-Jimenez C (2005) *Phyllobacterium catacumbae* sp. nov., a member of the order 'Rhizobiales' isolated from Roman catacombs. Int J Syst Evol Microbiol 55:1487–1490

Kanehisa M, Goto S (2000) KEGG: Kyoto Encyclopedia of Genes and Genomes. Nucleic Acids Res 28, 27-30

Kanehisa M (2019) Toward understanding the origin and evolution of cellular organisms. Protein Sci 28, 1947-1951

Kanehisa M, Sato Y, Morishima K (2016) BlastKOALA and GhostKOALA: KEGG tools for functional characterization of genome and metagenome sequences. J Mol Biol.428, 726-731

361 Knösel D (1962) Prüfung von Bakterien auf Fähigkeit zur Sternbildung. Zentralbl Bakteriol Parasitenkd
362 Infektionskr Hyg II Abt 116:79–100

363 Kumar S, Stecher G, Li M, Knyaz C, Tamura K (2018) MEGA X: Molecular Evolutionary Genetics Analysis
364 across computing platforms. Molecular Biology and Evolution 35:1547-1549

365 Lane DJ (1991) 16S/23S rRNA sequencing. In: Stackebrandt E, Goodfellow M (ed) Nucleic Acid
366 Techniques in Bacterial Systematics. Wiley, Chichester, pp 115–175

367 León-Barrios M, Ramírez-Bahena MH, Igual JM, Peix A, Velázquez E (2018) *Phyllobacterium*
368 *salinisoli* sp. nov., isolated from a *Lotus lancerottensis* root nodule in saline soil from Lanzarote. Int J
369 Syst Evol Microbiol 085–1089

370 Liang LX, Sun QW, Hui N, Zhang XX, Li LB, Liu L (2019) *Phyllobacterium phragmitis* sp. nov., an
371 endophytic bacterium isolated from *Phragmites australis* rhizome in Kumtag Desert. Antonie Van
372 Leeuwenhoek 112(5), 661-668. https://doi.org/10.1007/s10482-018-1195-5

373 Mantelin S, Saux MF, Zakhia F, Béna G, Bonneau S, Jeder H, Lajudie P, Cleyet-Marel JC (2006) Emended
374 description of the genus *Phyllobacterium* and description of four novel species associated with plant
375 roots: *Phyllobacterium bourgognense* sp. nov., *Phyllobacterium ifriqiyense* sp. nov., *Phyllobacterium*
376 *leguminum* sp. nov. and *Phyllobacterium brassicacearum* sp. nov. Int J Syst Evol Microbiol 56:827–839

377 Matsen FA et al (2010) pplacer: linear time maximum-likelihood and Bayesian phylogenetic placement
378 of sequences onto a fixed reference tree. BMC Bioinformatics 11:538

379 Mergaert J, Cnockaert MC, Swings J (2002) *Phyllobacterium myrsinacearum* (subjective synonym
380 *Phyllobacterium rubiacearum*) emend. Int J Syst Evol Microbiol 52:1821–1823

381 Miller LD, Russell MH, Alexandre G (2009) Diversity in bacterial chemotactic responses and niche
382 adaptation. Adv Appl Microbiol 66:53-75. DOI:10.1016/S0065-2164(08)00803-4

383 Muyzer G, Yildirim E, van Dongen U, Kühl M, Thar R (2005) Identification of '*Candidatus* Thioturbo
384 danicus,' a microaerophilic bacterium that builds conspicuous veils on sulfidic sediments. Appl Environ
385 Microbiol 71: 8929–8933. https://doi.org/10.1128/AEM.71.12.8929-8933.2005

386 Nielsen LP, Risgaard-Petersen N, Fossing H, Christensen PB, Sayama M (2010) Electric currents couple
387 spatially separated biogeochemical processes in marine sediment. Nature 463(7284), 1071–4.
388 https://doi.org/10.1038/nature08790

389 Parks DH, Imelfort M, Skennerton CT, Hugenholtz P, Tyson GW (2015) CheckM: assessing the quality
390 of microbial genomes recovered from isolates, single cells, and metagenomes. Genome Res
391 25(7):1043–1055. https://doi.org/10.1101/gr.186072.114

392 Parks DH et al (2018) A standardized bacterial taxonomy based on genome phylogeny substantially
393 revises the tree of life. Nature Biotechnol 36(10):996. https://doi.org/10.1038/nbt.4229

394 Pfeffer C, Larsen S, Song J, Dong M et al (2012). Filamentous bacteria transport electrons over
395 centimetre distances. Nature 491, 10–398 13. https://doi.org/10.1038/nature11586

396 Price MN, Dehal PS, Arkin AP (2009) FastTree: Computing Large Minimum-Evolution Trees with
397 Profiles instead of a Distance Matrix. Mol Biol Evol 26:1641-50. doi:10.1093/molbev/msp077

398 Price MN, Dehal PS, Arkin AP (2010) FastTree 2 – Approximately Maximum-Likelihood Trees for Large
399 Alignments. PLoS ONE 5(3): e9490. https://doi.org/10.1371/journal.pone.0009490

400 Rice CW, Hempfling WP (1978) Oxygen-limited continuous culture and respiratory energy
401 conservation in Escherichia coli. J Bacteriol 134 115–124

402 Richter M, Rosselló-Móra R (2009) Shifting the genomic gold standard for the prokaryotic species
403 definition. Proc Natl Acad Sci USA 106, 19126–19131. https://doi.org/10.1073/pnas.0906412106

404 Safronova VI, Sazanova AL, Kuznetsova IG, Belimov AA, Andronov EE, Chirak ER, Popova JP, Verkhozina
405 AV, Willems A, Tikhonovich IA (2018) *Phyllobacterium zundukense* sp. nov. a novel species of rhizobia

406 isolated from root nodules of the legume species *oxytropis triphylla* (pall.) pers. Int J Syst Evol
407 Microbiol 68:1644–1651

408 Sánchez M, Ramírez-Bahena MH, Peix A, Lorite MJ, Sanjuán J, Velázquez E, Monza J (2014)
409 *Phyllobacterium loti* sp. nov. isolated from nodules of *Lotus corniculatus*. Int J Syst Evol Microbiol
410 64:781–786

411 Schauer R, Risgaard-Petersen N, Kjeldsen KU, Bjerg JJT, Jørgensen BB, Schramm A, Nielsen LP (2014)
412 Succession of cable bacteria and electric currents in marine sediment. ISME J 8(6), 1314-1322

413 Scilipoti S, Koren K, Risgaard-Petersen N, Schramm A, Nielsen LP (2021) Oxygen consumption of
414 individual cable bacteria. Science Advances 7(7) eabe1870. DOI: 10.1126/sciadv.abe1870

415 Seemann T (2014) Prokka: rapid prokaryotic genome annotation. Bioinformatics 30(14):2068-9.
416 https://doi.org/10.1093/bioinformatics/btu153

417 Sievers F, Wilm A, Dineen DG, Gibson TJ, Karplus K, Li W, Lopez R, McWilliam H, Remmert M, Söding
418 J, Thompson JD, Higgins D (2011) Fast, scalable generation of high-quality protein multiple sequence
419 alignments using Clustal Omega. Mol Syst Biol 7: 539. doi:10.1038/msb.2011.75

420 Szurmant H, Bunn MW, Cannistraro VJ, Ordal GW (2003) *Bacillus subtilis* hydrolyzes CheY-P at the
421 location of its action, the flagellar switch. J Biol Chem 278:48611-6. DOI:10.1074/jbc.M306180200

422 Thar R, Fenchel T (2005) Survey of motile microaerophilic bacterial morphotypes in the oxygen-
423 gradient above a marine sulfidic sediment. Appl Environ Microbiol 71:3682-3691. DOI:
424 10.1128/AEM.71.7.3682-3691.2005

425 Thar R, Kühl M (2002) Conspicuous veils formed by vibrioid bacteria on sulfidic marine sediments. Appl
426 Environ Microbiol 68:6310-6320. DOI: 10.1128/AEM.68.12.6310-6320.2002

427 Thorup C, Petro C, Bøggild A, Ebsen TS, Brokjær S, Nielsen LP, Schramm A, Bjerg JJ (2021) How to grow
428 your cable bacteria: Establishment of a stable single-strain culture in sediment and proposal of
429 *Candidatus* Electronema aureum GS. Syst Appl Microbiol

430 Valverde A, Velázquez E, Fernández-Santos F, Vizcaíno N, Rivas R, Mateos PF, Martínez-Molina E, Igual
431 JM, Willems A (2005) *Phyllobacterium trifolii* sp. nov., nodulating *Trifolium* and *Lupinus* in Spanish soils.
432 Int J Syst Evol Microbiol 55:1985–1989

433 Wingett SW, Andrews S (2018) FastQ Screen: a tool for multigenome mapping and quality control.
434 F1000 Res 7:1338. https://doi.org/10.12688/f1000research.15931.2

Figures and tables

Table 1 **Differential characteristics of strain R2-JL^T (1, this study) compared to 8 closely related *Phyllobacterium* species.**

Species: (2) *P. myrsinacearum*, 14 strains; (3) *P. zundukense*, 4 strains; (4) *P. sophorae* CCBAU 03422^T; (5) *P. brassicacearum*, 2 strains; (6) *P. bourgognense*, 2 strains; (7) *P. trifolii*, 2 strains; (8) *P. endophyticum*, 2 strains. Data from Liang *et al.* 2019, León-Barrios *et al.* 2018, Jiao *et al.* 2015, Mantelin *et al.* 2006, Mergaert *et al.* 2002, Safronova *et al.* 2018, Sanchez *et al.* 2014, Valverde *et al.* 2005, Flores-Félix *et al.* 2013.

Similarity to R2-JL (%)	**1**	**2**	**3**	**4**	**5**	**6**	**7**	**8**
genome (FastANI)[a]	NA	92.64	80.89	80.22	80.07	79.86	79.80	78.42
16S rRNA gene (BLAST)[a]	NA	100	98.79	98.38	98.65	98.65	98.38	97.72
Characteristic								
isolation source[a]	Sed	Nod	Nod	Nod	Nod	Nod	Nod	Nod
growth at/on								
pH 6	+	*nr*	-	*nr*	+	+	*nr*	+
pH 5	+	+	-	*nr*	v	+	-	+
1% NaCl	+	v/+	v	+	v	+	v	+
2% NaCl	*nd*	+	*nr*	*nr*	w	-	+	*nr*
3% NaCl	*nd*	v/+	*nr*	*nr*	-	-	+	*nr*
4% NaCl	+	*nr*	*nr*	*nr*	*nr*	*nr*	*nr*	*nr*
acetic acid	+	+	+	-	v	-	v	v
α-D-lactose	+	-	*nr*	-	+	-	v	+
α-keto-glutaric acid	-	+	w/-	-	v	-	v	v
β-hydroxy-D,L-butyric acid	w	+	*nr*	+	-	+	+	-
β-methyl-D-glucoside	w	-	-	-	w/+	-	+	w/+
citric acid	+	+	-	-	-	-	v	-
dextrin	+	+	-	+	w/-	-	+	v
D-galactose	w	+	+	+	+	+	+	+
D-galacturonic acid	+	+	w/-	-	w/-	-	w	v
D-gluconic acid	-	+	w/-	-	v	v	-	v
D-glucose-6-PO4	-	+	*nr*	-	-	-	-	-
D-glucuronic acid	+	+	+	-[b]	w/-	-	-[b]	v
D-lactic acid methyl ester	-	+	w/-	+	-	+	+	-
D-melibiose	+	-	*nr*	*nr*	-	-	*nr*	+
D-raffinose	+	-	-[b]	-[b]	-	-	-[b]	v[b]
D-saccharic acid	-	-	-	*nr*	-	v	+	-
γ-amino-butyric acid	-	+	w/-	-	w	-	+	v
glucuronamide	+	-	*nr*	+	-	-	+	-
glycerol	-	+	+	-	+	-	+	+
inosine	-	+	-	-	-	-	-	-
L-alanine	+	+	-	-	v	v	w/-	v
L-aspartic acid	+	+	+	+	v	v	+	-
L-fucose	+	+	+	+	w/+	+	+	+
L-glutamic acid	+	+	+	+	-	-	+	-
L-histidine	+	v/-	-	+	v	-	+	+
L-lactic acid	-	+	+	+	+	+	+	-

L-serine	-	+	-	-	v	-	-	v
maltose asm	+	+	+	+	+	+	+	v
methyl pyruvate	-	*nr*	w/-	*nr*	+	*nr*	*nr*	+
N-acetyl-β-D-mannosamine	-	+	+	*nr*	-	*nr*	*nr*	+
N-acetyl-D-galactosamine	+	-	-	-	v	+	-	-
N-acetyl-D-glucosamine	+	+	*nr*	+	v	+	+	-
(potassium) gluconate asm	w	+	*nr*	*nr*	-	-	+	*nr*
propionic acid	-	v/-	w/+	-	w/-	-	-	-
quinic acid	-	v/+	w	+	+	v	+	v
sucrose	+	+	+	+	+	+	+	v
tween 40	w	-	+	-	-	-	-	-
urease	-	+	+	*nr*	+	+	w	-
acid produced from								
arabinose	w	v/+	*nr*	+[c]	+[c]	+[c]	+[c]	+
melibiose	-	-	-	-	-	-	-	+

442 NA, not applicable; Sed, microaerophilic veil *in* freshwater sediment; Nod, plant nodule; +, growth; -, no growth;

443 w, weak growth; v, (type) strain results are variable (v/#, # indicates the result of the type strain); nd, not

444 determined; nr, no data *reported;* asm, assimilation.

445 [a] values and source are based on the type strain of the species

446 [b] D/L not specified

447 [c] measured as L-arabinose

Figure legends

Figure 1

Fig 1 *Schematic and picture (50× magnification) of in-house developed and adapted "trench slide" sediment chamber and its use for capillary-based collection of veil bacteria. Scale bar 150 µm*

Figure 2

Fig 2 *Images of P. calauticae R2-JL^T. (A) Scanning electron micrograph of cells of strain R2-JL^T showing (sub) polar flagella, indicated with two arrows. Scale bar 1 µm. (B) Phase-contrast darkfield image with of strain R2-JL^T forming a veil, indicated by a purple bracket, at the oxic-anoxic interface. Scale bar 100 µm*

Figure 3

Fig 3 *Phylogenetic tree highlighting the placement of* Phyllobacterium calauticae *R2-JL^T (in bold) within the genus* Phyllobacterium. *Phylogenetic marker genes translated to protein sequences were identified in genomes available from NCBI with GTDB-Tk identify and alignment was subsequently performed with GTDB-Tk align. The maximum likelihood tree was inferred using FastTree2. Bootstrap support (1000 replicates) is shown as closed circles >99%, half open circles >85%, and open circles >60% likeliness.* Mesorhizobium loti *LMG 6125^T was used as outgroup to root the tree. Scale bar 0.04 substitutions per amino acid position*

Figures

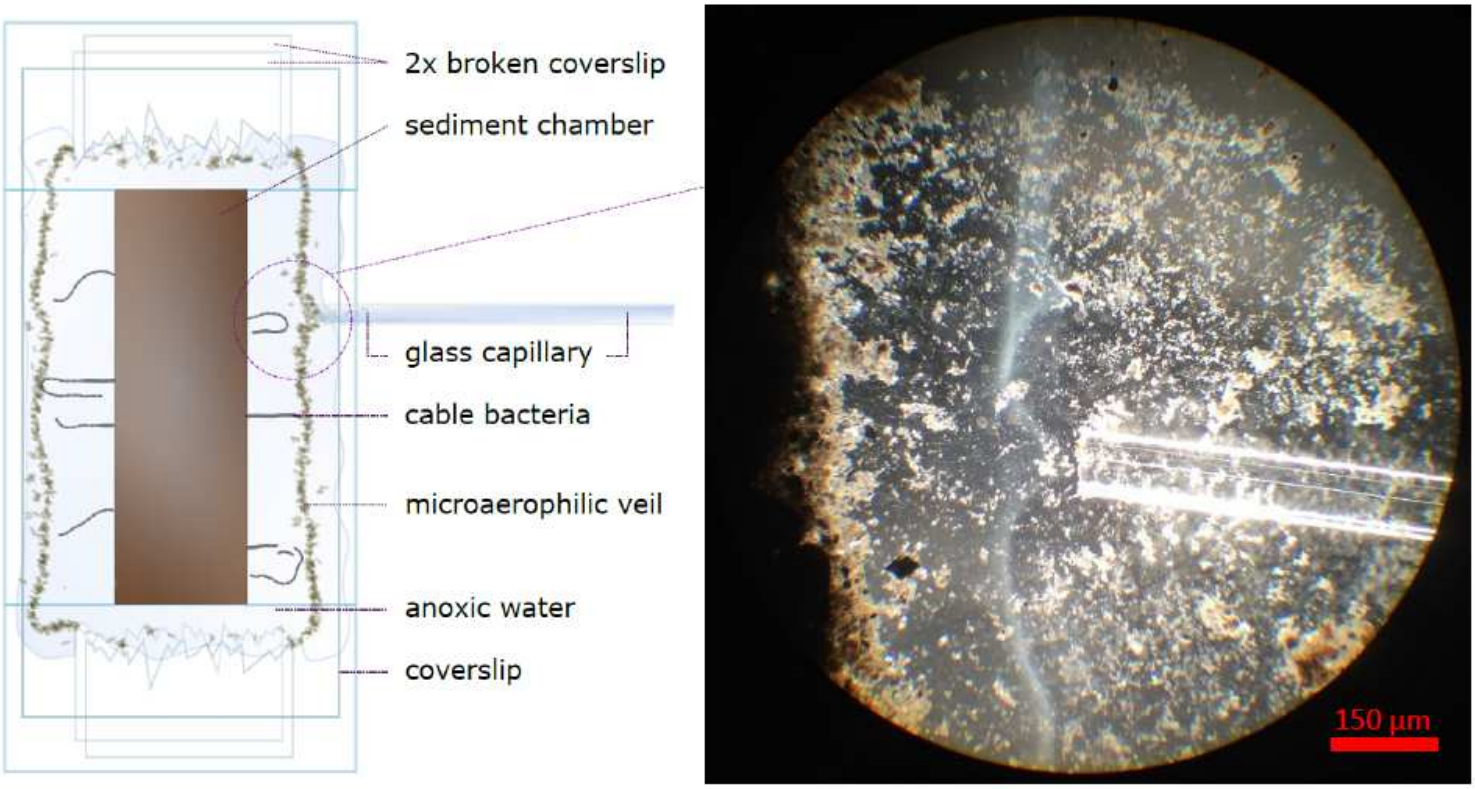

Figure 1

Schematic and picture (50× magnification) of in-house developed and adapted “trench slide” sediment chamber and its use for capillary-based collection of veil bacteria. Scale bar 150 µm

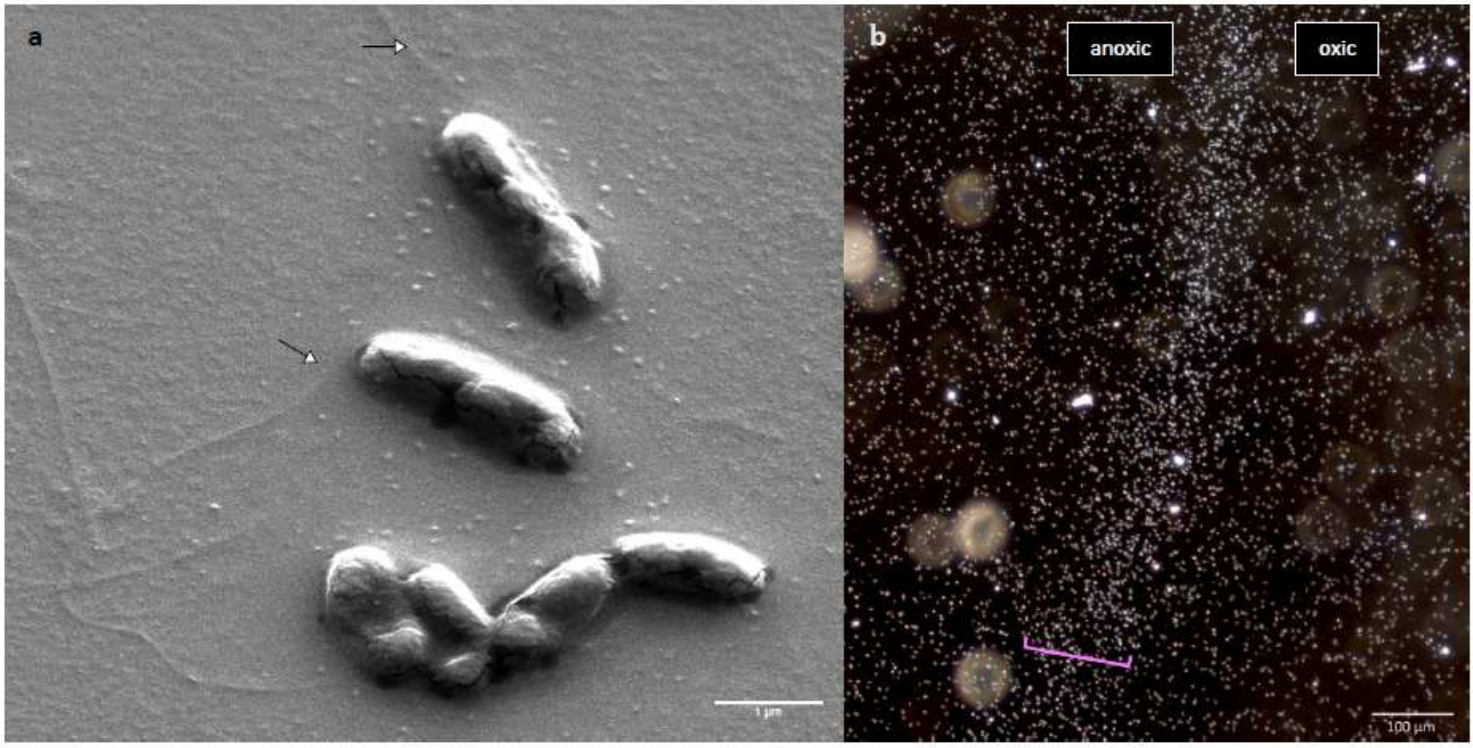

Figure 2

Images of P. calauticae R2-JLT. (A) Scanning electron micrograph of cells of strain R2-JLT showing (sub) polar flagella, indicated with two arrows. Scale bar 1 µm. (B) Phase-contrast darkfield image with of strain R2-JLT forming a veil, indicated by a purple bracket, at the oxic-anoxic interface. Scale bar 100 µm

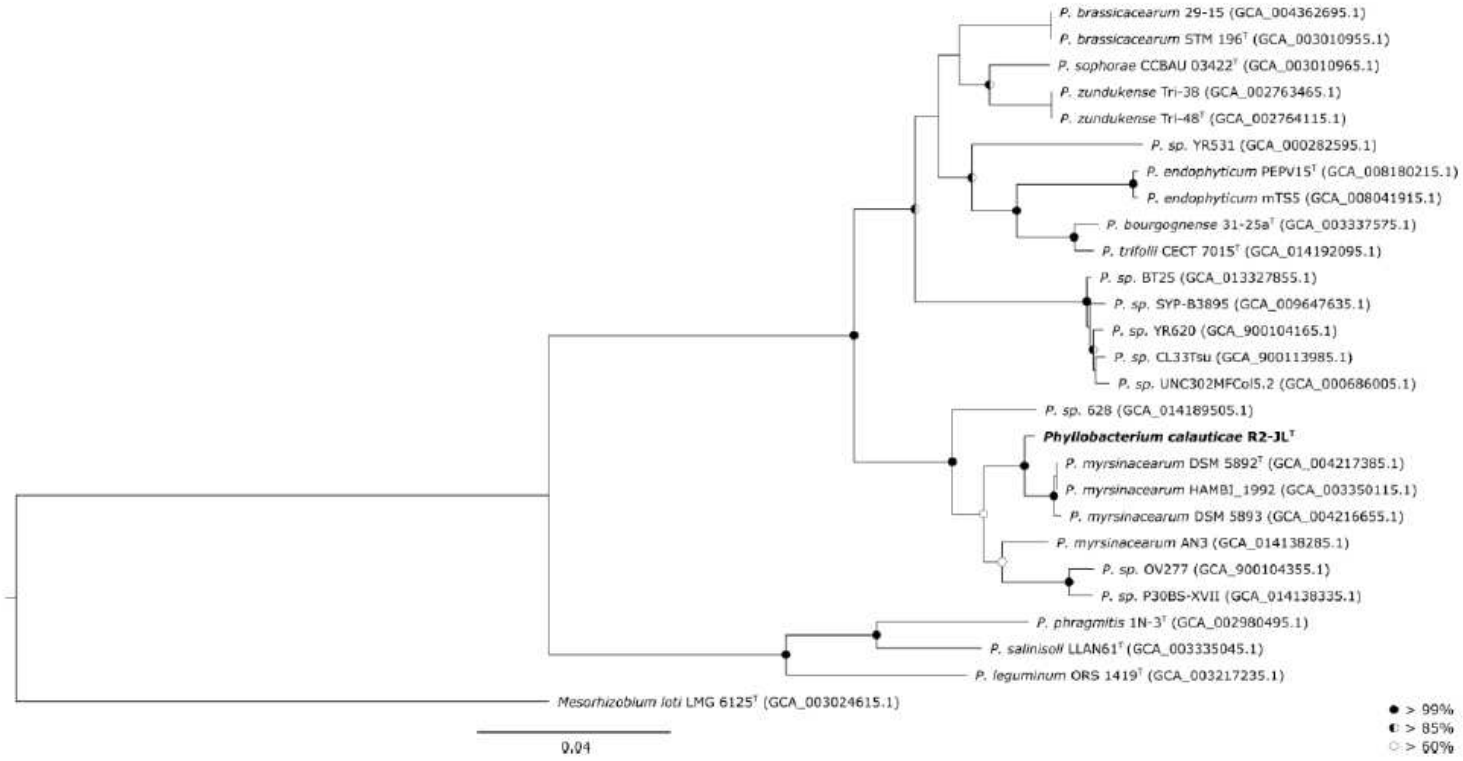

Figure 3

Phylogenetic tree highlighting the placement of Phyllobacterium calauticae R2-JLT (in bold) within the genus Phyllobacterium. Phylogenetic marker genes translated to protein sequences were identified in genomes available from NCBIwith GTDB-Tk identify and alignment was subsequently performed with GTDB-Tk align. The maximum likelihood tree was inferred using FastTree2. Bootstrap support (1000 replicates) is shown as closed circles >99%, half open circles >85%, and open circles >60% likeliness. Mesorhizobium loti LMG 6125T was used as outgroup to root the tree. Scale bar 0.04 substitutions per amino acid position

Supplementary Files

This is a list of supplementary files associated with this preprint. Click to download.

- SupplementaryInformationLustermans2021.pdf